Journal of Hazardous Materials 161 (2009) 787–799

Contents lists available at ScienceDirect

Journal of Hazardous Materials

journal homepage: www.elsevier.com/locate/jhazmat

Kinetics of *para*-nitrophenol and chemical oxygen demand removal from synthetic wastewater in an anaerobic migrating blanket reactor

Özlem Selçuk Kuşçu, Delia Teresa Sponza*

Dokuz Eylül University Engineering, Faculty Environmental Engineering Department, 35160 Izmir, Turkey

ARTICLE INFO

Article history:
Received 13 December 2007
Received in revised form 8 April 2008
Accepted 8 April 2008
Available online 22 April 2008

Keywords:
AMBR
Grau-kinetic
p-NP
Stover-Kincannon kinetic

ABSTRACT

A laboratory scale anaerobic migrating blanket reactor (AMBR) was operated at different HRTs (1–10.38 days) in order to determine the *para*-nitrophenol (*p*-NP) and COD removal kinetic constants. The reactor was fed with 40 mg L^{-1} *p*-NP and 3000 mg L^{-1} glucose-COD. Modified Stover-Kincannon and Grau second-order kinetic models were applied to the experimental data. The predicted *p*-NP and COD concentrations were calculated using the kinetic constants. It was found that these data were in better agreement with the observed ones in the modified Stover-Kincannon compared to Grau second-order model. The kinetic constants calculated according to Stover-Kincannon model are as follows: the saturation value constant (K_B) and maximum utilization rate constants (R_{max}) were found as 31.55 g COD L^{-1} day^{-1}, 29.49 g COD L^{-1} day^{-1} for COD removal and 0.428 g *p*-NP L^{-1} day^{-1}, 0.407 g *p*-NP L^{-1} day^{-1} for *p*-NP removal, respectively (R^2 = 1). The values of (a) and (b) were found to be 0.096 day and 1.071 (dimensionless) with high correlation coefficients of R^2 = 0.85 for COD removal. Kinetic constants for specific gas production rate were evaluated using modified Stover-Kincannon, Van der Meer and Heerrtjes and Chen and Hasminoto models. It was shown that Stover-Kincannon model is more appropriate for calculating the effluent COD, *p*-NP concentrations in AMBR compared to the other models. The maximum specific biogas production rate, G_{max}, and proportionality constant, G_B, were found to be 1666.7 mL L^{-1} day^{-1} and 2.83 (dimensionless), respectively in modified Stover-Kincannon gas model. The bacteria had low Haldane inhibition constants (K_{ID} = 14 and 23 mg L^{-1}) for *p*-NP concentrations higher than 40 mg L^{-1} while the half velocity constant (K_s) increased from 10 to 60 and 118 mg L^{-1} with increasing *p*-NP concentrations from 40 to 85 and 125 mg L^{-1}.

1. Introduction

The successful application of anaerobic technology for the treatment of industrial wastewater depends on the development of high-rate bioreactors. Among various anaerobic treatment systems, the anaerobic migrating blanket reactor (AMBR) was developed as a high-rate anaerobic treatment system that combines compartmentalization, continuous flow, short hydraulic retention time, simple design, no gas–liquid separation, no feed distribution system and no recycling to the reactor [1]. The studies related to AMBR include only the treatments of some industrial wastewaters such as synthetic wastewaters containing only dry milk substrate [1] and wastewaters containing sucrose as substrate [2].

Nitrophenols and nitroaromatic compounds are widely used as raw materials or intermediates in the manufacture of explosives, pharmaceuticals, pesticides, pigments, dyes, wood preservatives, leather and rubber chemicals [3]. *para*-Nitrophenol (*p*-NP) is toxic to plant, animal and human health [4]. It is a high-priority pollutant and poses significant health and environmental risk due to its mutagenic and carcinogen activities [5]. The purification of wastewaters contaminated with these pollutants is very difficult since they are resistant to conventional treatment techniques [5]. Although several investigators have used physical and chemical methods such as volatilization, photodegradation, photo-catalysis and advanced oxidation [6] to treat wastewater containing nitrophenol, anaerobic biodegradation is the ultimate degradation mechanism [7]. Under anaerobic conditions, nitrophenols are readily reduced to their corresponding amines. Under reductive methanogenic conditions, the nitroaromatic compounds are initially reduced to their respective amino derivatives [3]. In the reductive phase, *p*-NP degraded to *p*-aminophenol (*p*-AP) [8]. Some reports indicated that *p*-AP can be mineralized under methanogenic conditions [9]. Therefore, further degradation of aminophenols takes place via deamination to phenol [8,10] or by carboxylation and dehyroxylation to 3-aminobenzoate [8,11]. The study carried out by Karim and Gupta [8] indicated that *p*-AP is the only intermediate metabolite in the effluent measured from the *p*-NP degradation [8]. *p*-NP in low

* Corresponding author. Tel.: +90 232 4127119; fax: +90 232 4531143.
E-mail addresses: ozlem.selcuk@deu.edu.tr (Ö.S. Kuşçu), delya.sponza@deu.edu.tr (D.T. Sponza).

0304-3894/$ – see front matter © 2008 Elsevier B.V. All rights reserved.
doi:10.1016/j.jhazmat.2008.04.039

Nomenclature

a	$S_i/(k_{2(S)}X)$ (day)
A	total disc surface area (m^2)
b	constant for Grau second-order model (dimensionless)
dS/dt	substrate removal rate by time ($mg\,L^{-1}\,day^{-1}$)
E	efficiency
G	specific biogas production rate ($mL\,L^{-1}\,day^{-1}$)
G_B	proportionality constant (dimensionless)
G_{max}	maximum specific biogas production rate ($mL\,L^{-1}\,day^{-1}$)
k	Chen and Hasminoto kinetic constant (dimensionless)
$k_{2(S)}$	second-order substrate removal rate constant (day^{-1})
k_{sg}	Van der Meer and Heertjes kinetic constant ($mL\,mg^{-1}$)
K_B	saturation value constant ($g\,L^{-1}\,day^{-1}$)
M	specific methane production rate ($mL\,L^{-1}\,day^{-1}$)
M_B	proportionality constant (dimensionless)
M_{max}	maximum specific methane gas production rate ($mL\,L^{-1}\,day^{-1}$)
N_e	effluent *p*-NP concentration ($mg\,L^{-1}$)
N_i	influent *p*-NP concentration ($mg\,L^{-1}$)
OLR	organic loading rate ($g\,L^{-1}\,day^{-1}$)
Q	inflow rate ($L\,day^{-1}$)
R_{max}	maximum substrate removal rate ($g\,L^{-1}\,day^{-1}$)
S_i, S_e	substrate concentration in the feed and effluent ($g\,COD\,L^{-1}$ or $mg\,COD\,L^{-1}$)
V	reactor volume (L)
V_M	Van der Meer and Heertjes methane production ($mL\,day^{-1}$)
VSS	volatile suspended concentration ($g\,L^{-1}$)
X	concentration of biomass in the reactor ($g\,VSS\,L^{-1}$)
Y	actual methane yield ($L\,CH_4\,g^{-1}$VS added)
Y_{max}	ultimate methane yield $L\,CH_4\,g^{-1}$ VS added)
θ_H	hydraulic retention time (day)
μ_{max}	maximum specific growth rate of microorganisms (day^{-1})

concentrations is metabolized with the simultaneous utilization of primary substrate (COD) serving as the source of carbon and energy required for growth [2]. Xenobiotic compounds, such as nitrophenol, act as secondary substrate that do not contribute to the anabolic process leading to cell growth [12].

This compound poses a significant health risk since it has mutagenic and carcinogenic activities and may bioaccumulate in the food chain [13]. Among the nitrophenol; *p*-NP, 4-NP and 2,4-dinitrophenol (2,4-DNP) were listed on the US Environmental Protection Agency (EPA)'s as "Priority Pollutants" [13]. Therefore, knowledge of the kinetic of biodegradation is essential for evaluation of, the removal of organic pollutants such as *p*-NP as well as for prediction of bioreactor performance with respect to the degradation of toxic compound. The substrate kinetic models consist of the substrate consumption and microbial growth rates during operation of reactors under steady-state conditions. The models are used to control and predict the treatment plant operation performance and to optimize the plant design [14].

Since *p*-NP is a toxicant and a priority pollutant chemical [13,15] and its removal kinetic and relevant kinetic constants have not been determined before in AMBR reactor, this study was undertaken. The objectives of this study were: (1) to observe the performance of AMBR reactor through simultaneous utilization of *p*-NP and COD by methanogens, (2) to determine a kinetic model for an AMBR including the effluent COD and *p*-NP concentrations and relevant kinetic constants at different hydraulic retention times (HRTs), (3) to verify the validity of the models by comparing the experimental (observed) and predicted data at decreasing HRTs and (4) to determine a suitable kinetic model for biogas and methane productions in AMBR reactor.

2. Materials and methods

2.1. Experimental lab-scale reactor and seed

The AMBR reactor consisted of a rectangular tank (inside dimensions: length = 45 cm, height = 20 cm, width = 15 cm) with an active volume of 13.5 L, which was divided into three compartments. Round openings with a diameter of 2.5 cm from the rear of the stainless steel sheets separated the compartments. These openings were placed at the bottom to create sufficient contact between biomass and substrate. The three compartments were mixed equally every 15 min at 60 rpm to ensure gentle mixing. The flow over the horizontal plane of the reactor was reversed once a week. A weekly change in flow direction was chosen to prevent a pH drop due to VFA build up in the initial compartment and to prevent unequal biomass levels due to anticipated biomass migration between compartments. The samples were withdrawn from the AMBR reactor effluent after stopping the mixing process for 15 min. A schematic diagram of the lab-scale AMBR used in this study is presented in Fig. 1.

Partially granular anaerobic sludge was used as seed in the AMBR reactor and was obtained from an up-flow anaerobic sludge blanket reactor from the Pakmaya Yeast Beaker Factory in Izmir, Turkey. The total suspended solid (TSS) and volatile suspended solid (VSS) concentrations of the feed sludge were 45 and 35 $g\,L^{-1}$, respectively in AMBR. The specific methanogenic activity of the feed sludge was measured as 0.34 $g\,COD\,g^{-1}$ VSS day^{-1}.

2.2. Composition of synthetic wastewater

A constant *p*-NP concentration of 40 $mg\,L^{-1}$ was used in the feed wastewater together with glucose, giving a COD concentration of 3000 $mg\,L^{-1}$ during continuous operations of AMBR. Furthermore, Vanderbilt mineral salts medium was used to develop the microorganisms together with *p*-NP and glucose. The Vanderbilt mineral medium was prepared in distilled water by dissolving per liter 0.4 g $MgSO_4$, 0.4 g NH_4Cl, 0.4 g KCl, 0.3 g Na_2S, 0.08 g $(NH_4)_2HPO_4$, 0.05 g $CaCl_2$, 0.04 $FeCl_2$, 0,01 g $CoCl_2$, 0,01 g KI, 0.01 g $Na(PO_3)_6$, 0.5 mg $AlCl_3$, 0.5 mg $MnCl_2$, 0.5 mg $CuCl_2$,0.5 mg $ZnCl_2$, 0.5 mg NH_4VO_3, 0.5 mg $NaMoO_4$, 0.5 mg H_3BO_3, 0.5 mg $NiCl_2$, 0.5 mg $NaWO_4$, 0.5 mg Na_2SeO and 0.01 g cystein [16]. Anaerobic conditions were maintained by adding 0.5 $mg\,L^{-1}$ of sodium thioglycollate into the feed indicating the reductive conditions prevalent in anaerobic AMBR reactor. No vitamins or yeast-extract were added to the synthetic wastewater. Desired alkalinity and neutral pH were obtained by the addition of 5000 $mg\,L^{-1}$ $NaHCO_3$ into the feed media.

2.3. Operation conditions

AMBR reactor was operated with synthetic wastewater containing constant *p*-NP concentration of 40 $mg\,L^{-1}$ together with glucose during 186 days of continuous operation in order to investigate the COD and *p*-NP removal kinetics and biogas and methane productions kinetics of AMBR at six different hydraulic retention times. HRT was decreased progressively from 10.38 days to 5.19, 3.4,

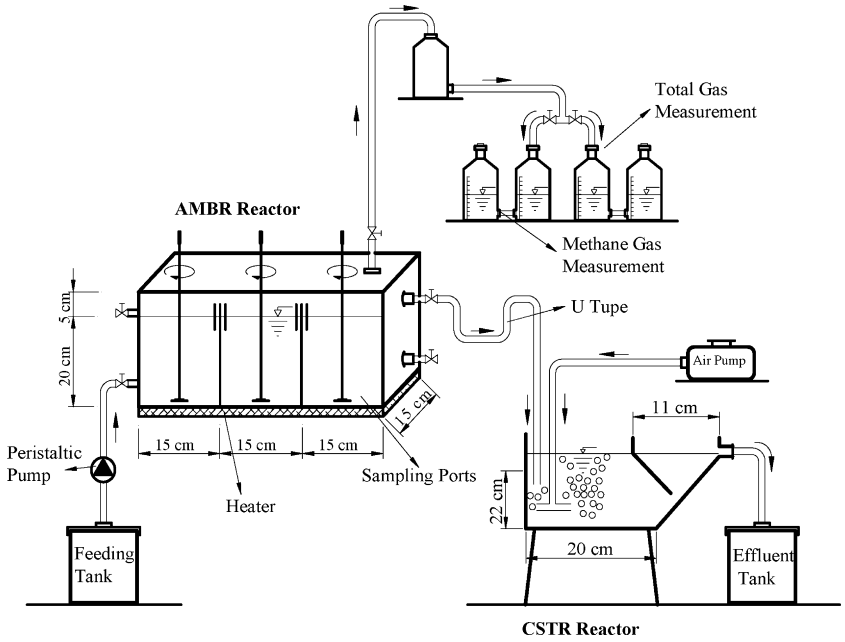

Fig. 1. Schematic diagram of lab-scale AMBR reactor.

2.4, 1.5–1 day in AMBR. The operating parameters for AMBR reactor through continuous operation are summarized in Table 1. The AMBR reactor was operated at steady-state conditions for approximately 25–35 days in every HRT. The HRTs were not decreased before reaching steady-state conditions in four consecutive days in order to observe the effect of HRT on COD, *p*-NP and biogas and methane production rates in AMBR reactor. No sludge wasting was applied in AMBR.

2.4. Analytical methods

TSS and VSS in the AMBR were measured by membrane filtration technique [17]. Soluble COD in influent and effluent samples was determined by closed reflux colorimetric method [17]. *p*-Nitrophenol was measured by using Tris–HCl acid at a wavelength of 400 nm in UV–vis spectrophotometer. The samples were centrifuged at 4000 rpm for 10 min and the absorbance values of supernatants were determined [5,18]. The *p*-nitrophenol was also measured in HPLC (HP, 2006) in order to check the difference between the methods [17]. A C18 column and a mobile phase in the ratios of 50:50:0.1 consisting from methanol:water:H_3PO_4 was used. The wavelength of the detector and detection limit were 254 nm and 0.03 mg mL^{-1}. No significant differences was observed between the results. Biogas and methane productions were measured with liquid displacement method. Biogas productions were measured by passing the gas through distilled water containing 2% (v/v) H_2SO_4 and 10% (w/v) NaCl [19]. Methane productions were measured by using distilled water containing 3% NaOH (w/v) [20]. Methane content in biogas was determined by Dräger (Stuttgart, Germany) Pac-Ex methane gas analyzer.

Bicarbonate alkalinity (Bic.Alk.) and total volatile fatty acid (TVFA) concentrations were measured simultaneously using titrimetric method proposed by Anderson and Yang [21].

2.5. Statistical analysis

The regression and multiple regression analysis between *y* (dependent) and *x* (independent) variables were carried out using Windows Excel data analysis (1998).

3. Kinetic approaches

In this study, two different substrate removal kinetic models, including Grau second-order and modified Stover-Kincannon, were used to determine the substrate removal kinetic constants. Modified Stover-Kincannon, Van der Meer and Heerrtjes and Chen and Hasminoto models were used to determined suitable specific total gas and methane gas productions.

3.1. Substrate removal kinetics

3.1.1. Modified Stover-Kincannon model

In modified Stover-Kincannon model, the substrate utilization rate is expressed as a function of the organic loading rate (OLR) by monomolecular kinetic for biofilm reactors such as rotating biological contactors and biological filters. A special feature of modified

Table 1
Operational conditions for AMBR reactor

Period	Days	HRT (day)	OLR (kg COD L^{-1} day^{-1})	Influent COD concentration (mg L^{-1})	Influent *p*-NP concentration (mg L^{-1})	*p*-NP loading rate (g *p*-NP m^{-3} day^{-1})
Run 1	35	10.38	0.31	3120	40	3.85
Run 2	33	5.19	0.60	3123	40	7.71
Run 3	27	3.4	0.93	3170	40	11.76
Run 4	34	2.4	1.31	3164	40	16.67
Run 5	32	1.5	2.14	3118	40	26.67
Run 6	25	1	3.25	3140	40	40

Stover-Kincannon model is the utilization of the concept of total organic loading rate as the major parameter to describe the kinetics of an AMBR reactor in terms of organic matter removal and methane production. In the modified Stover-Kincannon model if the maximum utilization rate (R_{max}) ($g\,L^{-1}\,day^{-1}$) and the saturation value constant (K_B) ($g\,L^{-1}\,day^{-1}$) values obtained from the removal of COD and *p*-NP were substituted in Eqs. (1)–(3) could be used to predict the effluent COD and *p*-NP concentrations, respectively [22].

$$Q\frac{S_i - S_e}{V} = \frac{R_{max} x Q S_i/V}{K_B + (QS_i/V)} \quad (1)$$

$$S_e = S_i - \frac{R_{max} S_i}{K_B + QS_i/V} \quad (2)$$

$$N_e = N_i - \frac{R_{max} N_i}{K_B + (QN_i/V)} \quad (3)$$

where (QS_i/V) explain the OLR applied to the reactor. Q and V are the inflow rate ($L\,day^{-1}$) and the volume of the anaerobic reactor (L), respectively S_e and S_i are effluent and influent COD concentrations ($mg\,COD\,L^{-1}$). N_i and N_e are influent and effluent *p*-NP concentrations ($mg\ p\text{-NP}\,L^{-1}$).

3.1.2. Grau second-order multicomponent substrate removal model

The general equation of a second-order kinetic model can expressed with Eqs. (4) and (5) in order to predict the effluent COD and *p*-NP concentrations [23,24].

$$S_e = S_i\left(1 - \frac{1}{b + a/\theta_H}\right) \quad (4)$$

$$N_e = N_i\left(1 - \frac{1}{b + a/\theta_H}\right) \quad (5)$$

where θ_H is the hydraulic retention time (day), a is equal to $S_i/(k_{2(S)}X)$ (day) and b is the constant (dimensionless). S_i and S_e express the influent and effluent substrate concentrations ($mg\,L^{-1}$).

3.2. Biogas and methane production kinetics

3.2.1. Modified Stover-Kincannon model

The biogas and methane gas production rates can also be mathematically modeled in terms of substrate removal. The biogas and methane gas productions and quality are dependent on the substrate removal and substrate-loading rate. The model developed by Stover (Eqs. (6) and (7)) can be used to determine the total gas and the specific methane gas production rates [25].

$$\frac{1}{G} = \frac{G_B}{G_{max}} \times \frac{1}{OLR} + \frac{1}{G_{max}} \quad (6)$$

$$\frac{1}{M} = \frac{M_B}{M_{max}} \times \frac{1}{OLR} + \frac{1}{M_{max}} \quad (7)$$

G is the specific biogas production rate ($mL\,L^{-1}\,day^{-1}$) and G_{max} is defined as the maximum specific biogas production rate ($mL\,L^{-1}\,day^{-1}$). G_B is the proportionality constant ($mg\,L^{-1}\,day^{-1}$) for biogas production. V_M is methane production ($mL\,day^{-1}$), Q is wastewater flow rate ($L\,day^{-1}$). S_i and S_e are explained as the influent and effluent substrate concentrations ($mg\,L^{-1}$), respectively.

3.2.2. Van der Meer and Heertjes model

The model developed by Van der Meer and Heertjes [26] (Eq. (8)) was applied to determine methane gas production. In this model the methane production is related to Van der Meer and Heertjes kinetic constant (k_{sg}) ($mL\,mg^{-1}$), with flowrate applied to AMBR and removal efficiency of substrate.

$$V_M = k_{sg} Q(S_i - S_e) \quad (8)$$

where k_{sg} is Chen and Hasminoto kinetic constant (dimensionless).

3.2.3. Chen and Hasminoto model

The ultimate methane yield (Y_{max}) is defined as liter of the methane produced per gram of volatile solids added as the hydraulic retention time reaches infinity [27]. Ultimate methane yield (Y_{max}) is usually determined by plotting the actual methane yield (Y) versus 1/HRT and extrapolating the curve to 1/HRT = 0. The biodegradable COD in the reactor will be directly proportional to ($Y_{max} - Y$), and Y_{max} will be directly proportional to the biodegradable COD loading [27]. In Chen and Hasminoto model the substrate removal is an indicator of biogas production in anaerobic process [22]. The actual methane yield (Y) and the maximum specific growth rate (μ_{max}) (day^{-1}) of the methanogens can be calculated using Eq. (9).

$$\frac{Y_{max}}{Y_{max}} - Y = \frac{\theta_H \times \mu_{max}}{k} + 1 - \frac{1}{k} \quad (9)$$

3.3. Inhibition kinetics of COD and p-NP

The most commonly used kinetic expression is that of Monod which relates the rates of substrate removal, and half saturation constant (K_s) (Eq. (10)) [28] (Table 2). Inhibition models are classified according to the effect of toxic compounds on the reaction rate (R_{max}), and half saturation constant (K_s) in equations derived from Eq. (14) (Eqs. (11)–(14)) [29]. Four inhibition functions ((Eqs. (11)–(14)) were fitted with the experimental data using Microsoft Office Excel 2003 (see Table 2). In Haldane kinetic, the inhibition affects the bacterial growth (μ) and the half saturation constant (K_s) [30]. In this kinetic non-linear regression technique was used by minimizing the residual sum of squares.

Table 2
Monod and some inhibition kinetic models

Kinetic	Kinetic function	
Monod kinetic	$-\frac{dS}{dt} = -R = \frac{R_{max} S}{K_s + S}$	(10)
Inhibition type	**Inhibition functions**	
Competitive inhibition	$-\frac{dS}{dt} = -R = -\frac{R_{max} S}{K_s(1 + I_D/K_{ID}) + S}$	(11)
Non-competitive inhibition	$-\frac{dS}{dt} = -R = -\frac{R_{max}}{(1 + K_s/S)(1 + I_D/K_{ID})}$	(12)
Uncompetitive inhibition	$-\frac{dS}{dt} = -R = -\frac{R_{max} S/(1 + I_D/K_{ID})}{K_s/(1 + I_D/K_{ID}) + S}$	(13)
Haldane inhibition	$-\frac{dS}{dt} = -R = -\frac{\mu_{max} S X}{(K_s + S + (S^2/K_{ID}))Y}$	(14)

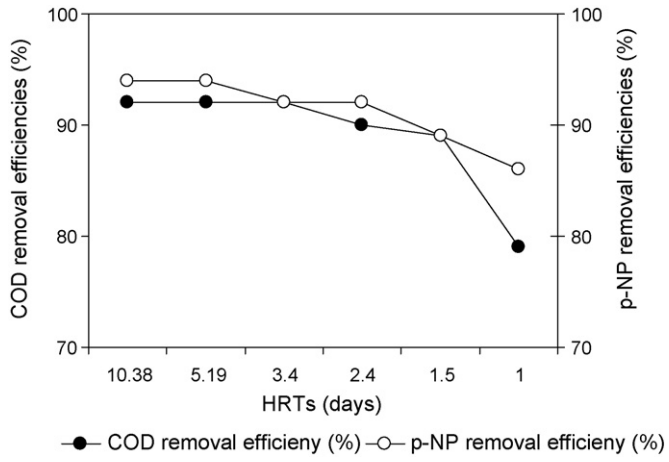

Fig. 2. COD and *p*-NP removal efficiencies at different HRTs in AMBR.

4. Results and discussion

4.1. Reactor performance

4.1.1. Effects of decreasing HRT on COD and p-NP removal efficiencies in anaerobic AMBR reactor

The effect of HRTs on the COD and *p*-NP removal efficiencies are shown in Fig. 2. 92% COD removal efficiency and 94% *p*-NP removal efficiencies were obtained at a HRT of 10.38 days corresponding to an OLR of 0.31 kg m^{-3} day^{-1} and *p*-NP loading rate of 3.85 g m^{-3} day^{-1}. The COD and *p*-NP removal efficiencies were stable between 92% and 94% until a HRT of 2.4 days, respectively. The COD and *p*-NP removal efficiencies were found as 79% and 86% at HRT of 1 day, respectively. The maximum COD (E = 90–92%) and *p*-NP (E = 92–94%) removal efficiencies were observed at HRTs varying between 2.4 and 10.38 days corresponding OLRs of 0.31–1.31 kg COD m^{-3} day^{-1} and *p*-NP loading rate of 3.85–16.6 g m^{-3} day^{-1}. The high *p*-NP removals depend on conversion of *p*-NP to their respective aromatic amines with the energy obtained from the glucose-COD via co-metabolism in AMBR reactor. In the study carried out by Tseng and Yang [31] an anaerobic biological fluidized bed was used to treat synthetic wastewater containing *p*-NP compounds [31]. The results proved that *p*-NP was the most toxic for methanogens and removed with 65% efficiency at an initial *p*-NP concentration of 30 mg L^{-1} and a HRT of 6 days. The study performed by Bhatti et al. [4] showed that the treatment of 500 mg L^{-1} *p*-NP was completely degraded at a hydraulic retention time of 11 h under facultative aerobic conditions [4]. Karim and Gupta [32] studied the biotransformation of nitrophenols in an up-flow anaerobic sludge blanked reactor (UASB) [27]. The removal of *p*-NP was more than 99% at HRTs varying between 12 and 30 h in a sequencing batch reactor [32].

In a study carried out by Melgoza and Buitrón [5] the degradation of 25 mg L^{-1} *p*-NP in a batch sequencing biofilter under sequential anaerobic/aerobic conditions was investigated [5]. After 230 days of operation, the *p*-NP removal efficiency was 94% at a reaction time of 11.5 h (8 h for the anaerobic phase and 3.5 h for the aerobic one). In our study the *p*-NP and COD removal efficiencies are of the same order of magnitude (approximately 92–94%) although the influent *p*-NP concentrations in our study are comparably higher than the study performed by Melgoza and Buitrón [5]. In another study nearly 95% biotransformation of *p*-NP to *p*-AP was observed at an initial *p*-NP concentration of 40 mg L^{-1} in AMBR reactor [15] while 90% *p*-NP was converted to *p*-AP at *p*-NP concentration of 25 mg L^{-1} [15].

The results obtained in this study are considerably higher than the data obtained by Karim and Gupta [32] in an up-flow anaerobic sludge blanket reactor at an influent *p*-NP concentration of 30 mg L^{-1} (E = 88% *p*-NP removal efficiency) at a HRT of 1.2 days [32].

As the HRT decreased to 0.5 days the *p*-NP removal efficiency declined to 76%. In another study performed by Donlon et al. [33] 99% *p*-NP removal efficiency was obtained at an organic loading rate of 11.4 g COD L^{-1} day^{-1} and *p*-NP loading rate of 910 mg L^{-1} day^{-1} in an up-flow anaerobic sludge blanket reactor [33]. Uberoi and Bhattacharya [3] found that 20 mg L^{-1} 4-NP and 2-NP was removed with 95% efficiencies in an up-flow biofilm reactor following 25 days of acclimation period [3]. Melgoza and Buitrón [5] studied the degradation of *p*-NP in an anaerobic/aerobic process combined into a single reactor [5]. After 230 days of operation, the *p*-NP removal efficiency was 98% through reaction time of 11.5 h (8 h for the anaerobic phase and 3.5 h for the aerobic one).

4.1.2. Effect of decreasing HRT on the biogas and the methane gas productions in AMBR reactor

The variations of the biogas, methane gas productions and methane content (%) in AMBR are shown in Fig. 3 for all HRTs. From this figure, it can be seen that the daily biogas and methane gas productions increased whenever HRTs were decreased. However, methane gas percentages decreased with decreasing HRT. The daily biogas and methane gas productions increased from 2.16 to 12.25 L day^{-1} and from 1.015 to 3.8 L day^{-1}, respectively, when the HRTs were decreased from 10.38 to 1 day. However, the methane gas percentage decreased from 47% to 31% at low HRTs. Although acidogenesis is prominent compared to methanogenesis at low HRTs, in this study a process imbalance is not apparent in AMBR. If the rate of acid formation exceeds the rate of breakdown to methane, a process imbalance results with decreases in methane contents of biogas. In the study performed by Karim and Gupta [32] the methane gas percentage was 38–50% at an initial p-NP concentration of 30 mg L^{-1} and at OLRs varying between 2.04 and 4.02 kg COD m^{-3} day^{-1} m^3 day in an up-flow anaerobic sludge blanket reactor [32]. Since the anaerobic treatment of a wastewater is directly related to the amount of methane produced, the amount of methane generated per kilogram of COD stabilized should be taken as an indicator for determining the stabilization degree of *p*-NP and COD. In this study, the methane yields were found between 0.116 and 0.209 L CH_4 g^{-1} VS added (0.264 and 0.01 m^3 CH_4 kg^{-1} COD removed) (see Table 2). Part of the glucose-COD degraded to VFA such as acetic acid via acidification resulting in methane production. The remaining COD was used as carbon source for

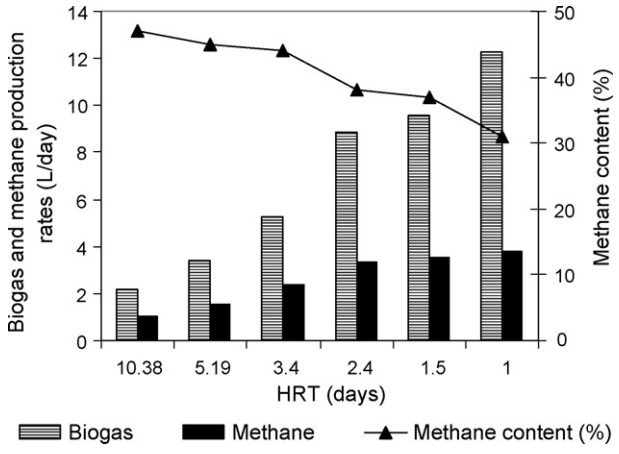

Fig. 3. The variations of the biogas, methane gas and methane content (%) in AMBR.

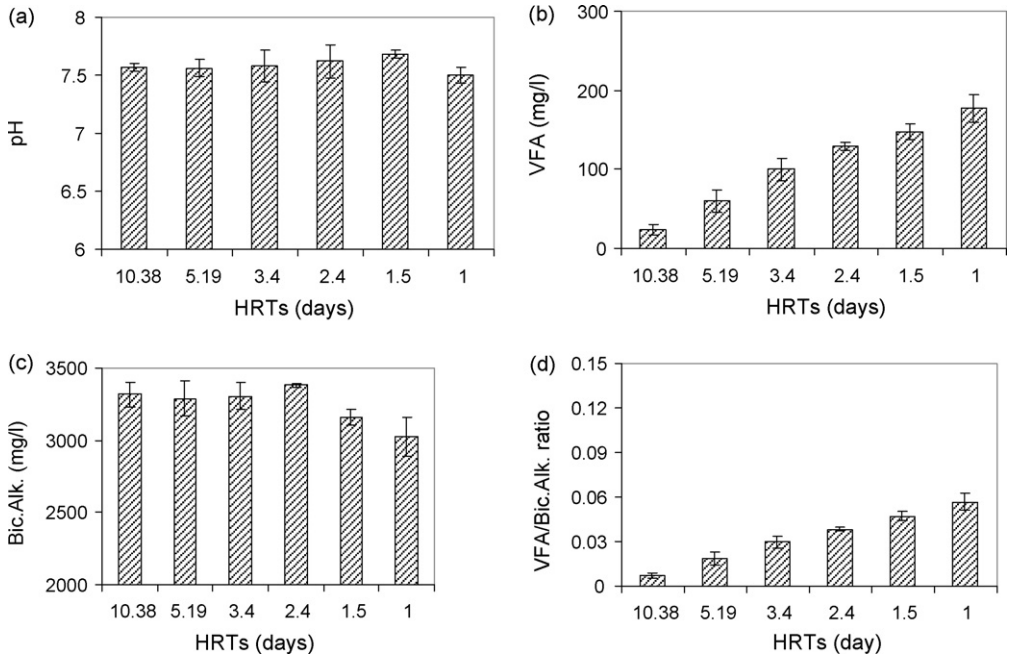

Fig. 4. The effluent pH (a), VFA (b), Bic.Alk. (c) and VFA/Bic.Alk. ratios (d) at different HRTs.

the biodegradation of *p*-NP to *p*-aminophenol and for growth of methanogens [34]. The methane yield results obtained in this study are lower than those obtained by Kuscu and Sponza [34] in an anaerobic baffled reactor (ABR) treating 10–700 mg L^{-1} *p*-NP. Kuscu and Sponza [34] found that the methane yield decreased from 0.34 to 0.28 m^3 CH_4 kg^{-1} COD, when the *p*-NP loading rates increased from 9.7 to 67.9 g m^{-3} day^{-1} in an ABR reactor [34]. Karim and Gupta [32] found that the methane gas production decreased from approximately 0.22 to 0.12 m^3 CH_4 kg^{-1} COD removed with increase of *p*-NP loading rate from 0.023 to 0.06 g L^{-1} day^{-1} [32]. These results exhibit similar data to this study since all systems treat a toxic compound "*p*-NP".

4.1.3. Effects of HRTs on pH, total volatile fatty acid, bicarbonate alkalinity and TVFA/Bic.Alk. variations in AMBR reactor

The variations of pH, TVFA concentration, Bic.Alk. and TVFA/Bic.Alk. ratios in the effluent of AMBR are shown in Fig. 4 for all HRTs. The pH values varied between 7.5 and 7.8 in the effluent samples of AMBR for all HRTs. These data are between optimum pH values (pH 6.5 and 8.3) for anaerobic degradation [16]. The TVFA concentration in the effluent increased from 25 to 182 mg L^{-1} as the HRT decreased from 10.38 to 1 day corresponding to OLR of 0.31–3.25 kg m^{-3} day^{-1}. In a study performed by Kuscu and Sponza [34] all the TVFAs could be removed by an ABR until an OLR of 1.28 kg m^{-3} day^{-1} [34]. After this OLR, TVFA concentration in the effluent increased and was measured as 560 mg L^{-1} at an OLR of 3.16 kg m^{-3} day^{-1}. This showed that the AMBR reactor operated more efficiently than the ABR reactor. Since the VFA would be converted to methane gas, its accumulation is very important in terms of AMBR performance. The TVFA concentrations measured in this study were between 30 and 180 mg L^{-1} while the TVFA concentrations were 1100 mg L^{-1} at a HRT of 3 days and an initial *p*-NP concentration of 30 mg L^{-1} in the study performed by Karim and Gupta [32]. In their study the effluent TVFA concentration decreased to 228 mg L^{-1} when the *p*-NP removal efficiency was 98–99%. The stability of the anaerobic reactor is related to TVFA/Bic.Alk. ratio. If the TVFA/Bic.Alk. ratio is lower than 0.4, the reactor is stable. When the VFA/Bic.Alk. ratio is lower than 0.8, the reactor system is moderately stable or unstable as reported by Behling et al. [35]. In this study, the TVFA/Bic.Alk. ratios were found to be lower than 0.4 in the compartments and the effluent samples of AMBR at all HRTs.

4.2. Determination of kinetic coefficients for substrate removal models

Out of all the models used it was found that modified Stover-Kincannon and Grau second-order substrate kinetic models were more appropriate than the other models when the experimental data obtained from six different HRTs was applied to aforementioned models through the continuous operation of the AMBR. Some operation parameters and the experimental data obtained for influent and effluent COD, *p*-NP, VSSs and methane yields (*Y*) are shown in Table 3 for different HRTs.

Table 3
Experimental data obtained from different HRTs

V (L)	*Q* (L day^{-1})	HRT (day)	COD concentration (mg L^{-1})		*p*-NP concentration (mg L^{-1})		VSS (g L^{-1})	Methane yield (Y)	
			Influent (S_i)	Effluent (S_e)	Influent (N_i)	Effluent (N_e)		L CH_4 g^{-1} VSS added	L CH_4 g^{-1} COD removed
13.5	1.3	10.38	3170	240	40	2.4	40	0.116	0.264
13.5	2.6	5.19	3123	243	40	2.4	46	0.124	0.209
13.5	4	3.4	3170	269	40	3.2	50	0.141	0.209
13.5	5.64	2.4	3164	330	40	3.2	55	0.161	0.205
13.5	9.1	1.5	3118	384	40	4.4	58	0.177	0.135
13.5	12.8	1	3140	530	40	5.6	58	0.209	0.01

Table 4
Comparison of the kinetic constants according to Grau second-order and Stover-Kincannon models

Model	Kinetic constants	Values	
		COD removal	*p*-NP removal
Stover-Kincannon model	R_{max} (g L^{-1} day^{-1})	29.49	0.407
	K_B	31.55	0.428
	(g L^{-1} day^{-1})	$R^2 = 1$	$R^2 = 1$
		$y = 1.0696x + 0.00339$	$y = 1.023x + 2.455$
Grau second order	a (day)	0.0958	0.0967
	b (dimensionless)	1.071	1.096
	$k_{2(S)}$	0.654	0.0082
	(day^{-1})	$R^2 = 0.85$	$R^2 = 0.83$
		$y = 2.0531x - 1.005$	$y = 1.071x + 0.0856$

4.2.1. Substrate removal kinetics

4.2.1.1. Modified Stover-Kincannon model. Since the plot of $V/(QS_i)$ versus $V/Q(S_i - S_e)$ was linear, the intercept and slope of straight line on graph show $1/R_{max}$ and K_B/R_{max}, respectively using Eq. (1). From the slope and intercept of a best-fit line ($R^2 = 1$), maximum utilization rate (R_{max}) and saturation value constant (K_B) for COD removal were determined as 29.49 and 31.55 g COD L^{-1} day^{-1}, respectively with high regression coefficient ($R^2 = 1$; $y = 1.0696x + 0.00339$). The maximum substrate utilization rates (R_{max}) for COD was found as 16.38 and 19.22 g COD L^{-1} day^{-1} in the kinetic studies performed by Karim and Gupta [32,36] and Melgoza and Buitrón [5,32,36]. This showed that the present study exhibits higher maximum COD utilization rates. The effluent COD concentration can be predicted by using Eq. (2). Similarly, when the experimental data obtained from the *p*-NP removal was placed into Stover-Kincannon model (Eq. (3)), the R_{max} and K_B values were obtained as 0.407 and 0.428 g *p*-NP L^{-1} day^{-1}, respectively, with high regression coefficient ($R^2 = 1$, $y = 1.023x + 2.4551$). The maximum substrate utilization rates (R_{max}) for *p*-NP was found as 0.099 and 0.201 g *p*-NP L^{-1} day^{-1} by the kinetic studies performed by Karim and Gupta [32,36] and Melgoza and Buitrón [5,32,36]. These results are significantly lower than the present study. Stover-Kincannon model suggests that the substrate removal rates (COD and *p*-NP) are affected by the organic loading rate entering the reactor as described in Eqs. (2) and (3).

4.2.1.2. Grau second-order model. Kinetic coefficients (a, b and $k_{2(S)}$) in Grau second-order multicomponent model is determined in Eqs. (4) and (5). The values of (a) and (b) were calculated from the intercept and slope of the straight line on the graph. The values of (a) and (b) were found to be 0.096 day, 1.071 (dimensionless) with lower correlation coefficients of $R^2 = 0.85$ ($y = 2.053x + 1.005$) for COD removal compared to Stover-Kincannon kinetic. Grau second-order maximum substrate removal rate $k_{2(S)}$, was found as 0.654 day^{-1} through COD removal. The values of a, b and $k_{2(S)}$ were found as 0.0967 day, 1.0967 (dimensionless) and 0.0082 day^{-1} with lower correlation coefficient of ($R^2 = 0.83$, $y = 1.071x + 0.0856$) through *p*-NP removal in AMBR reactor. If a and b kinetic constants were substituted in Eqs. (4) and (5), the effluent COD and *p*-NP concentrations could be predicted using these equations, for Grau second-order model. The effluent substrate concentration or substrate removal efficiency is related to influent substrate concentration and Grau second-order kinetic constant.

4.2.1.3. Model testing. The kinetic constants determined from both models are summarized in Table 4. Stover-Kincannon model is used to determine the effluent substrate concentration for a given volume of an AMBR and influent substrate concentrations. The regression coefficient is higher in Stover-Kincannon kinetic model compared to Grau second-order model. Furthermore, the kinetic constants determined in Stover-Kincannon model are more meaningful than those observed in Grau model. The maximum substrate utilization rate (R_{max}) is higher and the saturation value constant (K_B) is lower during COD and *p*-NP removals. High COD and *p*-NP utilization rates increase the reactor efficiency while low substrate saturation constant indicates the utilization of both COD and *p*-NP by the methanogens in the AMBR. R_{max} value obtained from the study performed by Karim and Gupta [36] was 15.5 mg L^{-1} day^{-1} in an up-flow anaerobic sludge blanket reactor treating 30 mg L^{-1} of *p*-NP at a NP loading rate of 180 mg *p*-NP L^{-1} day^{-1} [36]. This result is significantly lower than the R_{max} value obtained from the present study. Low saturation values show that there is no accumulation of COD and *p*-NP in the anaerobic reactor resulting in high affinity of substrate to the methanogens (a), (b) and $k_{2(S)}$ kinetic constants calculated from the Grau model showed that (a) kinetic constant depends on influent COD, *p*-NP concentrations and that it was influenced by the inverse of second-order substrate removal rate constant and microorganism concentration. The (a) kinetic constant of 0.096 day will be increased with initial substrate concentration while it will be decreased as the second-order substrate removal rate and microorganism concentration increases. The maximum substrate removal rate constant $k_{2(S)}$ will be increased as the COD and *p*-NP removal efficiencies increases.

In order to test the validity of the models the results obtained from the experimental analysis (observed values) were compared with the values obtained from the models (predicted values). The actual and predicted values for the effluent COD and *p*-NP concentrations are shown in Table 5. As can be seen from this table, the predicted values were very close to the experimental results when Stover-Kincannon model was applied to the AMBR. The effluent COD and *p*-NP values predicted in Grau second-order model did not show such a good agreement with the results obtained from the experimental studies. Figs. 5 and 6 show the observed and predicted values in effluent for COD and *p*-NP.

A good linear relationship was obtained between observed effluent COD and *p*-NP concentrations obtained from the experiments carried out under six different HRTs and predicted COD, *p*-NP effluent concentrations were calculated by using the Eqs. (2) and (3) in modified Stover-Kincannon kinetic ($y = 1.309x - 98.69$

Table 5
Comparison of predicted and experimental (observed) results for modified Stover-Kincannon and Grau second-order kinetic model

HRT (day)	Experimental (observed) effluent COD and *p*-NP concentration (mg L^{-1})		Predicted effluent COD and *p*-NP concentration (mg L^{-1})			
			Stover-Kincannon		Grau second order	
	COD	*p*-NP	COD	*p*-NP	COD	*p*-NP
10.38	240	2.4	239	2.3	210	2.9
5.19	243	2.4	262	2.64	256	4.14
3.4	269	3.2	296	2.99	286	4.45
2.4	330	3.2	329	3.39	320	4.82
1.5	384	4.4	389	4.22	389	6.1
1	530	5.6	462	5.06	410	6.37

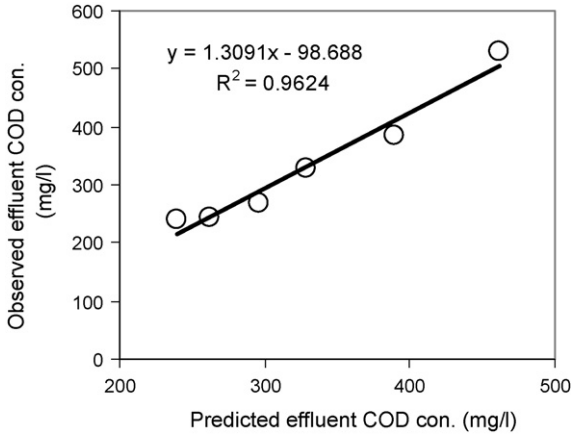

Fig. 5. The observed effluent COD concentration and predicted effluent COD in Stover-Kincannon kinetic model.

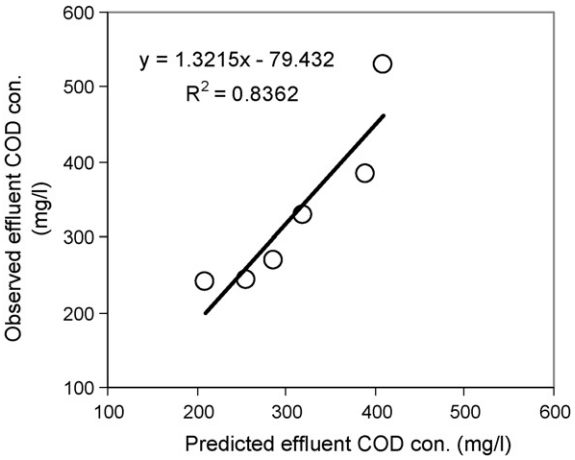

Fig. 7. The observed and predicted effluent COD concentrations in Grau second-order kinetic model.

and $R^2 = 0.96$, and $y = 1.188x–0.5463$ and $R^2 = 0.97$, respectively, for COD and *p*-NP) (see Figs. 5 and 6). The linear relationship between predicted and observed effluent COD, *p*-NP concentrations and predicted effluent COD, *p*-NP concentrations calculated from the Eqs. (5) and (6) in Grau second-order kinetic ($y = 1.3215x–79.432$, $R^2 = 0.83$; $y = 0.887x–0.7212$ and, $R^2 = 0.83$) respectively for COD and *p*-NP were lower than those obtained from the modified Stover-Kincannon model (see Figs. 7 and 8). The HRT versus observed and predicted effluent COD and *p*-NP concentrations clearly showed that the predicted effluent COD and *p*-NP concentrations were closer to the observed values when the calculated kinetic constants were placed into Stover-Kincannon kinetic model (see Table 5). If the AMBR reactor was operated between HRTs of 1.5 and 6 days the COD and *p*-NP removal efficiencies were 87–90% and 88–95%, respectively (see Fig. 2).

4.2.2. Biogas production kinetics

The kinetic constants obtained from three models were evaluated for biogas production in AMBR reactor.

4.2.2.1. Modified Stover-Kincannon model. In order to determine the kinetic coefficients (G_{max} and M_{max}) Eqs. (6) and (7) was used to measure total and methane gas productions in AMBR. The reciprocal of specific gas production ($1/G$) versus reciprocal of applied substrate-loading rates ($1/OLR$) were plotted in order to determine the kinetic constants relevant to biogas and methane gas productions, respectively. The intercept and slope of the best line resulted in $1/G_{max}$ and G_B/G_{max}, respectively. The maximum specific total gas production rate, G_{max}, and proportionality constant, G_B, were found to be 1666.7 mL L^{-1} day^{-1} and 2.83 (dimensionless), respectively ($R^2 = 0.97$; $y = 0.0017x + 0.0006$) using Eq. (6). The maximum methane gas production rate, M_{max}, and proportionality constant, M_B, were found to be 476.2 mL L^{-1} day^{-1} and 1.67 (dimensionless), respectively ($R^2 = 0.98$, $y = 0.0035x + 0.0021$) using Eq. (7). The specific biogas and methane gas production rates were predicted using Eqs. (6) and (7). In the modified Stover-Kincannon biogas kinetic model gas productions are related to gas production rates, applied organic loads and proportionality constants.

4.2.2.2. Van der Meer and Heertjes model. Eq. (9) was used to describe the kinetic constant (k_{sg}) in Van der Meer and Heertjes model. Kinetic constant, k_{sg}, was determined empirically from the slope of the line plotted between $Q(S_0 - S)$ and CH_4 ($R^2 = 0.83$, $y = 0.0947x + 1069.2$). The kinetic constant of gas production (k_{sg}) was found as 0.0947 mL CH_4 mg^{-1} COD removed. The methane gas productions were found between 361 and 3164 mL day^{-1} at HRTs varied from 10.38 to 1 day according to Eq. (9). In this model the

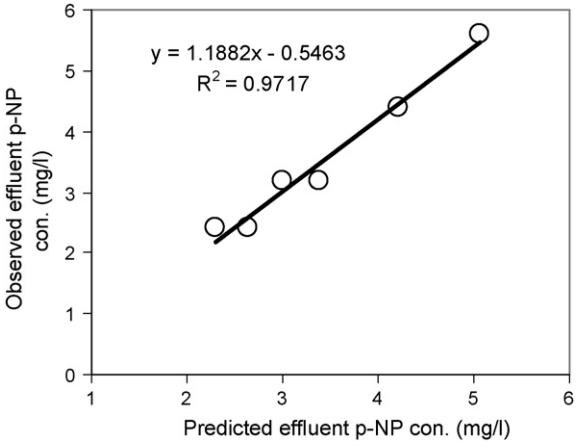

Fig. 6. The observed and predicted effluent *p*-NP concentrations in Stover-Kincannon kinetic model.

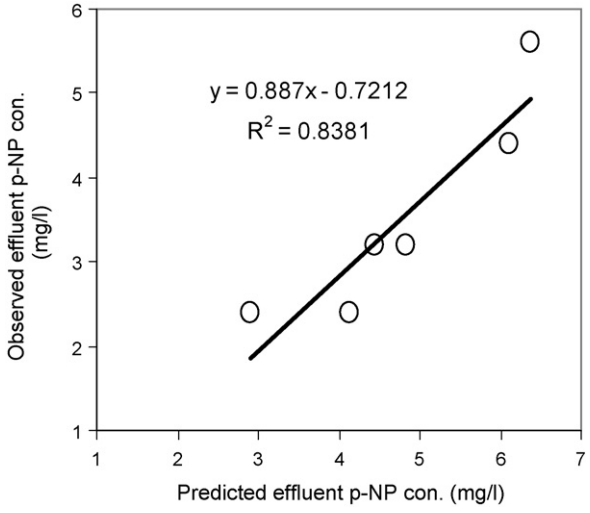

Fig. 8. The observed and predicted effluent *p*-NP concentrations in Grau second-order kinetic model.

Table 6
Comparison of kinetic constants for modified Stover-Kincannon, Van der Meer and Heertjes and Chen and Hasminoto models for total and methane gas productions

Model	Kinetic constants	Values	
		Methane gas production	Total gas production
Modified Stover-Kincannon model	G_{max} (mL L^{-1} day^{-1})	–	1666.7
	G_B (dimensionless)	–	2.83
	M_{max} (mL L^{-1} day^{-1})	476.2	–
	M_B (dimensionless)	1.67	–
		$R^2 = 0.98$	$R^2 = 0.97$
		$y = 0.0035x + 0.0021$	$y = 0.0017x + 0.0006$
Van der Meer and Heertjes model	k_{sg} (mL CH_4 mg^{-1} COD removed)	0.0947	–
		$R^2 = 0.83$	–
		$y = 0.0947x + 1069.2$	
Chen and Hasminoto model	Y_{max}	0.0704 L CH_4 g^{-1} VSS added or (0.283 L CH_4 kg^{-1} COD removed)	–
	μ_{max}	0.579 day^{-1}	–
	k (dimensionless)	0.164	–
		$R^2 = 0.68$	–
		$y = 3.531x–5.0974$	

methane gas production is related to gas kinetic constant, flowrate applied to the AMBR reactor and removed substrate concentrations.

4.2.2.3. Chen and Hasminoto model. The ultimate methane yield (Y_{max}) was calculated as 0.0704 L CH_4 g^{-1} VS added (0.283 L CH_4 kg^{-1} COD removed) from the intercept plotted between methane yield and 1/HRT ($R^2 = 0.68$, $y = 3.531x–5.097$) The maximum specific growth rate (μ_{max}) and k can be determined graphically by plotting the term ($Y_{max}/(Y_{max} - Y)$ versus HRT (Eq. (9)). The slope of the straight line is equal to μ_{max}/k and the intercept is equal to ($1–1/k$). The maximum specific growth rate (μ_{max}) was found as 0.579 day^{-1} and Chen and Hasminoto kinetic constant (k) was found as 0.164 (dimensionless) ($R^2 = 0.68$, $y = 3.531x–5.0974$). In this model, ultimate methane yield and maximum specific growth rate of methanogens were affected by hydraulic retention time and Chen and Hasminoto kinetic.

4.2.2.4. Model testing. The methane and biogas productions calculated from the experimental studies were compared in three different kinetic models. The kinetic constants calculated from the models are summarized in Table 6. The results for observed and predicted total and methane gas productions are given in Table 7. The total and methane gas productions predicted from the modified Stover-Kincannon model were very close to the observed data compared to the other two models at six different HRTs. The linear relationships showed that the regression coefficient is higher in modified Stover-Kincannon model compared to the other two models (see Table 5). Furthermore the kinetic constants relevant to gas production rates and the proportionality constants found from this model are meaningful for maximum anaerobic total and methane gas production rates [16]. The specific methane gas production rate is a third of the specific biogas production rate. This is in agreement with the findings obtained in Fig. 3, in which the methane gas productions are a third of the biogas productions for HRTs between 1 and 2.4 days.

The kinetic constant for methane gas production (k_{sg}) in Van der Meer and Heertjes Model was lower, indicating that the methane gas produced from the COD removed does not show the real data since the methane yields were calculated at between 0.116 and 0.209 CH_4 L g^{-1} VS added (0.264 and 0.01 CH_4 L kg^{-1} COD removed, respectively) to the AMBR from the observed studies (see Table 3). The observed methane gas production varied between 980 and 3800 mL day^{-1} which agrees with the data obtained from the modified Stover-Kincannon kinetic model and with the observed results (see Table 7). The ultimate methane yield (Y_{max}) is lower according to methane yields mentioned in Table 3 and the maximum growth rate for methanogens (μ_{max}) is significantly higher compared with the growth rates mentioned for anaerobic bacteria in Chen and Hasminoto model [16].

A good linear relationship was observed between methane gas productions obtained from the experiments carried out under six different HRTs and predicted methane gas productions calculated using the Eq. (7) in modified Stover-Kincannon model ($y = 0.9568x + 78.074$, $R^2 = 0.97$) (see Fig. 9). The linear relationship between observed and predicted effluent methane gas productions calculated using Eq. (8) was found to be lower ($y = 0.785x–602.45$, $R^2 = 0.83$) in Van der Meer and Heertjes model compared to modified Stover-Kincannon model (see Fig. 10). Similarly, the linear relationship between predicted and observed effluent methane gas productions and predicted methane gas calculated from the Eq. (9) in Chen and Hasminoto model was found to be lower ($y = 3.5863–4.236$, $R^2 = 0.52$) in, for example, Van der Meer and Heertjes model compared to modified Stover-Kincannon model (see Fig. 11). As a result, it was shown that the regression coeffi-

Table 7
Comparison of predicted and experimental (observed) results for total and methane gas productions in three model

HRT (day)	Experimental (observed) total and methane gas productions (mL day^{-1})		Predicted total and methane gas productions (mL day^{-1})			
			Modified Stover-Kincannon model		Van der Meer and Heertjes model	Chen and Hasminoto model
	Biogas	Methane	Biogas	Methane	Biogas	Methane
10.38	2,160	980	2,157	979	361	976
5.19	3,420	1560	3,936	1699	709	1,805
3.4	5,280	2370	5,565	2299	1099	2,541
2.4	8,840	3360	7,157	2826	1514	3,017
1.5	9,600	3552	9,532	3558	2356	6,864
1	12,000	3800	11,834	4197	3164	16,080

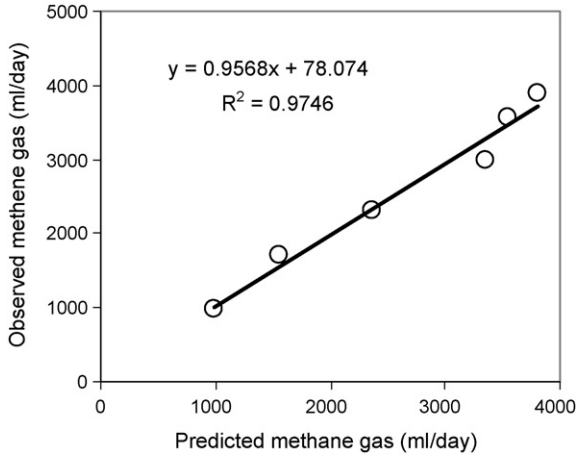

Fig. 9. The observed and predicted daily methane gas productions for modified Stover-Kincannon model.

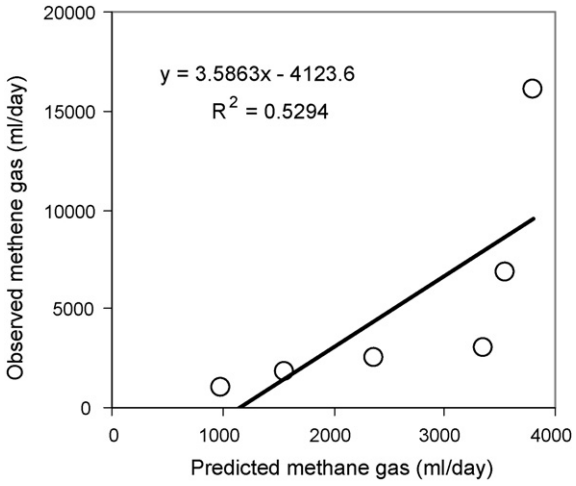

Fig. 11. The observed and predicted daily methane gas productions for Chen and Hasminoto model.

cients between predicted and observed methane gas productions is higher in Stover-Kincannon kinetic ($R^2 = 0.97$). Therefore, the observed and predicted methane gas productions in every HRTs were compared for three kinetic models (see Table 6). The HRT versus observed and predicted effluent methane gas productions showed that the predicted effluent methane gases are closer to the observed values when the calculated kinetic constants were placed into Stover-Kincannon kinetic model. If the AMBR reactor is operated at between HRTs of 1 and 10.38 days, the methane gas percentages will be between 35% and 45%, respectively, for long-term steady-state operations.

4.3. Inhibition kinetics for COD and p-NP

When $1/R$ is plotted against $1/S$, a straight line is obtained (Lineweaver–Burk plot) in Eq. (10). This line will have a slope of K_s/R_{max}, an intercept of $1/R_{max}$ on the $1/R$ axis, and an intercept of $-1/K_s$ on the $1/S$ axis. Such a double reciprocal plot has the advantage of allowing much more accurate determination of R_{max} and K_s. The double reciprocal plot can also give valuable information on inhibition. The possible effects of increasing *p*-NP concentrations on Lineweaver–Burk plot can be seen by the linearization of Eqs. (11)–(13). As summarized in Table 8, the parameters estimated using integrated Monod kinetic are, 0.62 day^{-1} for the maximum specific growth rate (μ_{max}), 210 $mg\,L^{-1}$ for the half saturation constant (K_s) and 37 $g\,L^{-1}\,day^{-1}$ for the maximum substrate removals rate (R_{max}) through anaerobic degradation of 3000 $mg\,L^{-1}$ glucose-COD without *p*-NP. Subsequently the initial (R_{max}) and K_s values were substituted into the integrated competitive, non-competitive and uncompetitive equations to obtain the relationships between K_s, K_{ID} and R_{max} at increasing *p*-NP concentrations from 40 to 125 $mg\,L^{-1}$. μ_{max} and K_s values were placed in integrated Monod equations to determine μ_{max}, K_s and K_{ID} values in Haldane kinetic. The results of this step showed that the Haldane equation gave the correct fit since the model fitted the experimental data very well with an r^2 greater than 99%. In the presence of *p*-NP the maximum specific growth rates (μ_{max}), varied in the range of 0.020 day^{-1} and 0.00009 day^{-1} for *p*-NP concentrations 40–125 $mg\,L^{-1}$ while the half saturation constant (K_s) increased from 10 to 118 mg *p*-NP L^{-1} for anaerobic degradation of 40–125 mg *p*-NP L^{-1} at a glucose-COD concentration of 3000 $mg\,L^{-1}$. The K_s, K_{ID} and μ_{max} for *p*-NP and COD were tabulated in Table 7. The calculated R_{max} values are unreastically high in competitive, non-competitive, and uncompetitive inhibition kinetics as seen in Table 8. For this reason Eqs. (11)–(13) has to be rejected. The threshold limitations for Haldane inhibitions are: $K_s \leq K_{ID}$; $K_s \leq 2000\ mg\,L^{-1}$; $\mu \leq \mu_{max} \leq 3\,\mu \leq$ for 3000 $mg\,L^{-1}$ glucose-COD; $K_s \leq K_{ID}$; $K_s \leq 20$ mg *p*-NP L^{-1} for 40–125 mg *p*-NP L^{-1} and $\mu \leq \mu_{max} \leq 3\,\mu \leq$ for *p*-NP degradation. The kinetic results relevant to COD and *p*-NP are given in Table 8 for Haldane equation.

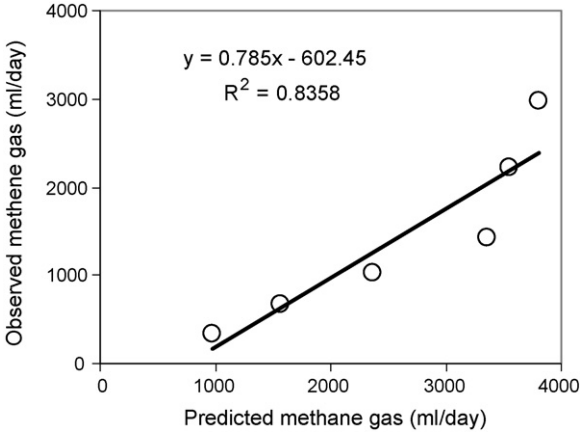

Fig. 10. The observed and predicted daily methane gas productions for Van der Meer and Heertjes model.

The inhibition coefficient (K_{ID}) decreased with 23 and 14 mg/l at *p*-NF concentrations of 85 and 125 mg/l. No inhibition of *p*-NP to bacterial cells was observed at 40 $mg\,L^{-1}$ *p*-NP concentration. These findings were in accordance with reports described by She et al. [37], though the data was slightly higher than corresponding μ_{max} and K_s values [37]. 4NP-specific removal rates observed in the study performed by Haghighi et al. were 1.3–2.7 d^{-1}, for a 4NP concentration of 10 $mg\,L^{-1}$, are significantly higher than that evaluated by She et al. (0.26–0.58 d^{-1}) at the same 4NP concentration [37]. The estimated M_{max}, K_s and K_{ID} constants were 20–26 d^{-1}, 1–7.7 $mg\,L^{-1}$ 4-NP and 0.89–8.9 $mg\,L^{-1}$, respectively, in a study performed by Haghighi et al. at a 4NP concentration of 30 $mg\,L^{-1}$ [38]. Table 7 shows that the inhibition coefficient (K_{ID}) decreased as the *p*-NP concentration increased from 40 to 125 $mg\,L^{-1}$. From this data, it can be concluded that the *p*-NP inhibition occurs between 85 and 125 $mg\,L^{-1}$. Because the inhibition effect is inversely proportional to the inhibition constant it will decrease as the toxicant concentration increases. The half saturation constant (K_s) reflects the fact that the K_s values of 4–5 $mg\,L^{-1}$

Table 8
Maximum specific growth rate, half velocity constant and inhibition coefficients in inhibition kinetics for glucose-COD and *p*-NP

p-NP concentrations	Type of inhibition	μ_{max} (day^{-1})[a] R_{max} ($g\,L^{-1}\,day^{-1}$) Glucose-COD	K_s ($mg\,L^{-1}$) Glucose-COD	K_{ID} ($mg\,L^{-1}$) Glucose-COD	μ_{max} (day^{-1})[a] R_{max} ($g\,L^{-1}\,day^{-1}$) *p*-NP	K_s ($mg\,L^{-1}$) *p*-NP	K_{ID} ($mg\,L^{-1}$ l) *p*-NP
0	No-inhibition (Monod kinetic)	0.60 [a]37 $R^2 = 0.97$	210	–	–	–	–
40	Competitive	[a]35	12.000	7800	[a]0.23	49	11
40	Non-competitive	[a]89 $R^2 = 0.74$	15.000	9700	[a]0.65	0.1	8
40	Un-competitive	[a]67 $R^2 = 0.77$	123	10.000	[a]2.34	0.7	1
40	Haldane inhibition	**0.23** $R^2 = 0.999$	**560**	**320**	**0.002**	**5**	**43**
85	Competitive	[a]87 $R^2 = 0.47$	25.000	6700	[a]0.99	50	13
85	Non-competitive	[a]56 $R^2 = 0.57$	34.000	4530	[a]0.89	0.9	82
85	Un-competitive	[a]45 $R^2 = 0.73$	300	4000	[a]1.22	11	09
85	Haldane inhibition	**0.10** $R^2 = 0.999$	**1200**	**112**	**0.0001**	**45**	**23**
125	Competitive	[a]21 $R^2 = 0.75$	2.000	4500	[a]1.4	45	89
125	Non-competitive	[a]76 $R^2 = 0.67$	13.000	2490	[a]1.6	43	99
125	Un-competitive	[a]45 $R^2 = 0.59$	450	23.000	[a]2.4	56	129
125	Haldane inhibition	**0.004** $R^2 = 0.999$	**2000**	**56**	**0.00009**	**120**	**14**

[a] R_{max} is used in Monod kinetic, competitive, non-competitive and un-competitive inhibitions. μ_{max} is used in Haldane inhibition.

imply that there is a strongly affinity for bacteria to bind the substrate. The half saturation constant (K_s) increases from 4 to 45 and 120 $mg\,L^{-1}$ in the presence of 85 and 125 $mg\,L^{-1}$ *p*-NP.

5. Evaluation of substrate, gas kinetics and inhibition models

The kinetic data showed that the Stover-Kincannon substrate removal kinetic model was more an appropriate model compared to the Grau second-order kinetic model for predicting the performance of the lab-scale AMBR reactor treating *p*-NP with glucose-COD as co-substrate. The substrate removal rate of this model is related to the total substrate loading applied to the AMBR reactor. The maximum substrate utilization rate (R_{max}) is higher for COD (29.49 $g\,L^{-1}\,day^{-1}$) and for *p*-NP (0.407 $g\,L^{-1}\,day^{-1}$) in Stover-Kincannon kinetic model (see Table 4). On the other hand, the saturation value constant (K_B) is lower during COD and *p*-NP removals. K_B is lower compared to the initial COD concentration of 3000 $mg\,L^{-1}$ and initial *p*-NP concentration of 40 $mg\,L^{-1}$ in Stover-Kincannon kinetic model. In this study the K_B values are lower (31.55 and 0.428 $g\,L^{-1}\,day^{-1}$ for COD and *p*-NP, respectively) under anaerobic conditions indicating the consumption of 2970 $mg\,L^{-1}$ of COD by the methanogens and the reduction of 40 $mg\,L^{-1}$ *p*-NP to 28 $mg\,L^{-1}$ *p*-AP [16]. The lower K_B value indicates the affinity of anaerobic microorganisms for the substrate. Therefore, it can be said that no COD and *p*-NP accumulation was observed in the AMBR reactor. The maximum substrate utilization rate (R_{max}) in Stover-Kincannon kinetic model is significantly higher than the Grau second-order substrate removal rate constant ($k_{2(S)}$) through *p*-NP and COD removals (0.654 day^{-1} and 0.0082 day^{-1}, respectively) (see Table 4). The kinetic constants indicated that the *p*-NP and COD were removed faster according to Stover-Kincannon kinetic than that of Grau second-order reaction kinetic.

Since the effluent COD and *p*-NP concentrations varied with HRT, these two parameters are the most important variables in the AMBR reactor. Therefore the observed effluent COD and *p*-NP concentrations and predicted effluent COD and *p*-NP concentrations for every HRT were compared for both substrate kinetic models. The predicted and observed COD and *p*-NP concentrations indicate that there is a high regression coefficient between these parameters in Stover-Kincannon kinetic compared to Grau second-order kinetic model (see Table 4). The regression coefficient between predicted and observed values for COD and *p*-NP were high ($R^2 = 1$ for both substrates) in Stover-Kincannon model compared to Grau second-order kinetic model ($R^2 = 0.85$ and 0.83, respectively for COD and *p*-NP). It can be concluded that the COD and *p*-NP in the AMBR reactor could be removed with high efficiencies according to Stover-Kincannon kinetic for long-term steady-state operations at HRTs varying between 1 and 10.38 days.

Very little kinetic data for 4-NP biodegradation and inhibition is reported in the specialized literature and a direct comparison is difficult and not completely reliable due to different models employed for data correlation. Finally, it is worth noting that kinetic parameters obtained in the present study are very close to those reported by Tomei et al. [39] who found $k_{max} = 2.2–4.6\ d^{-1}$, $K_s = 20\ mg\,L^{-1}$ 4-NP and $K_{ID} = 12\ mg\,L^{-1}$. 4-NP in kinetic tests carried out on biomass acclimated to a mixed feed of 4-NP and biogenic substrate [39]. A study performed by Zonglian et al. [40] showed that the K_s values is 7555, 7 $mg\,L^{-1}$ and K_{ID} value is 25.6 $mg\,L^{-1}$ at 2,4-NP concentrations higher than 45 $mg\,L^{-1}$ [40]. Podeh et al. [41] determined that 4-NP was efficiently degraded for a concentration of 49 $mg\,L^{-1}$ while inhibition was observed for *p*-NP concentrations higher than 67 $mg\,L^{-1}$ in a SBR reactor (K_s 55 $mg\,L^{-1}$ 4-NP and $K_{ID} = 15\ mg\,L^{-1}$) [41]. Tomei et al. [39] found that the Haldane equation as proposed by Andrew could be used to determine the inhibition kinetic of 4-NP in the range of 320 and 400 $mg\,L^{-1}$ [39]. In their study the K_s values increased from 16 to 39 $mg\,L^{-1}$ and the K_{ID} values decreased from 31 to 24 $mg\,L^{-1}$. In the present study, no inhibition was observed for *p*-NP concentration below 43 $mg\,L^{-1}$ for *p*-NP concentration of 85 and 125 $mg\,L^{-1}$ a serious inhibition was determined.

Higher K_s and lower K_{ID} values, in the Haldane inhibition, can be characterized as a system with low affinity to substrate and with

more inhibition. Low values of K_{ID} in *p*-PN higher than 43 mg L^{-1} indicates high inhibition potential because K_{ID} is in the denominator in the Haldane inhibition equation. Lower K_{ID} in samples containing high concentrations of *p*-NP (80–125 mg L^{-1}), represent the degree to which the microorganisms are significantly inhibited by increasing *p*-NP concentrations compared to low concentrations of the *p*-NP.

The maximum methane gas production is a quarter (M_{max} = 476.2 L day^{-1}) of the maximum specific biogas production (G_{max} = 1666.7 L day^{-1}) in Stover-Kincannon gas model. These results were found at HRTs lower than 5.19 days (see Table 6). At higher HRTs such as 5.19 and 10.38 days the maximum methane gas production is half of the maximum specific biogas production in Stover-Kincannon gas model (see Table 7). Proportionality constant for maximum specific biogas (G_B) was 2.83 (dimensionless), while the proportionality constant, for specific maximum methane gas production (M_B) was found to be 1.67 (dimensionless). The proportionally constant for methane gas is half of the biogas. Higher proportionally constant values for total and methane gas productions indicate that higher methane and total productions occurred in the removed substrates (COD and *p*-NP) in modified Stover-Kincannon model.

The observed and predicted methane gas productions showed that the predicted gas productions in modified Stover-Kincannon model are very close to the data obtained from the experimental studies (see Table 7). In the other words, the predicted data did not show a good agreement with the results obtained from the experimental studies in the two remaining models. The kinetic constant for gas production (k_{sg}) is lower (0.0947 mL methane mg^{-1} COD removed) for anaerobic gas production treating *p*-NP in Van der Meer and Heertjes Model [16,34]. On the other hand methane production rates (M = 361 and 3164 mL day^{-1}) versus HRTs showed a good agreement with the experimental studies in Van der Meer and Heertjes gas Model. The ultimate methane yield (Y_{max}) was found to be 0.074 L CH_4 g^{-1} VSS added and μ_{max} was 0.579 day^{-1} in Chen and Hasminoto gas model. These values are higher for anaerobic methanogens [16]. They should be between 0.01–0.09 L CH_4 g^{-1} VSS added and 0.12–0.24 day^{-1}, respectively [16]. The kinetic constant for Chen and Hasminoto model, k = 0.164 (dimensionless) is also higher for anaerobic bacteria [16].

6. Conclusions

The results of this study showed that synthetic wastewater containing *p*-NP could be treated effectively with an AMBR reactor at different HRTs varying between 1 and 10.38 days. The COD and *p*-NP removal efficiencies were stable at between 92% and 94% for HRTs 2.4 and 10.38 days. Daily total and methane gas productions in AMBR increased from 2160 to 12250 mL day^{-1} and from 1015 to 3800 mL day^{-1}, respectively with decreasing HRTs from 10.38 to 1 day. Methane content decreased from 47% to 31% as the HRT decreased to 1 from 10.38 days. The TVFA concentrations in effluent of the AMBR also increased from 25 to 182 mg L^{-1} as the HRT decreased from 10.38 to 1 day.

It was found that modified Stover-Kincannon kinetic model with high correlation coefficients (R^2 = 1) was more suitable for COD and *p*-NP removal in AMBR compared to Grau second-order kinetic model. The data predicted in Stover-Kincannon model showed a good agreement with the experimental results. The effluent substrate concentration in AMBR depends on maximum substrate removal rate (R_{max}), influent substrate concentration and saturation value constant (K_B) for glucose-COD and *p*-NP in Stover-Kincannon kinetic model. The maximum substrate utilization rate (R_{max}) is higher in this model indicating the high substrate removals at short retention times. Low saturation values (K_B) show that there is no accumulation of COD and *p*-NP in the anaerobic reactor resulting in high affinity of substrate to the methanogens.

Substantial inhibitory effects on K_s and K_{ID} values were observed, as evidenced by a decrease in K_{ID} values for *p*-NP higher than 43 mg L^{-1} in Haldane inhibition. There was no effect on half velocity constant and maximum specific growth rate up to a *p*-NP concentration of 43 mg L^{-1}. As the *p*-NP concentration increased to 120 mg L^{-1} the K_s value increased to 120 mg L^{-1}.

The modified Stover-Kincannon, Van der Meer and Heertjes model and Chen and Hasminoto gas models showed that the gas kinetic constants are more meaningful and the regression coefficient are higher in modified Stover-Kincannon model than the other two models. Therefore, the modified Stover-Kincannon gas model could be used to predict the methane gas productions in an AMBR treating *p*-NP. In this gas kinetic model, the total and methane gas productions are related to maximum specific and methane gas production rates, proportionality constant and OLR applied to the AMBR reactor.

For the aforementioned reasons, the kinetic studies carried out in the laboratory scale AMBR reactor showed that the modified Stover-Kincannon kinetic model can be used to better predict the treatment performance of a full-scale AMBR reactor for the treatment of wastewaters containing *p*-NP. Similarly, the same kinetic model can be used to better predict the biogas and methane gas productions in a full-scale AMBR reactor.

Acknowledgments

This study was executed as a part of the research activities of the Environmental Microbiology Laboratory of Environmental Engineering Department of project numbered 103 Y 106, which was funded by the Turkish Scientific Research Foundation (TÜBİTAK). The authors would like to thank this body for the financial support given to this project.

References

[1] T.L. Angenent, G.C. Banik, S. Sung, Anaerobic migrating blanket reactor treatment of low-strength wastewater at low temperatures, Water Environ. Res. 73 (5) (2001) 567–574.
[2] T.L. Angenent, S.J. Abel, S. Sung, Effect of an organic shock load on the stability of an anaerobic migrating blanket reactor, J. Environ. Eng. 128 (12) (2002) 1109–1120.
[3] V. Uberoi, S.K. Bhattacharya, Toxicity and degradability of nitrophenols in anaerobic systems, Water Environ. Res. 69 (1997) 146–156.
[4] I. Bhatti, H. Toda, K. Furukawa, *p*-Nitrophenol degradation by activated sludge attached on nonwoven, Water Res. 36 (2002) 1135–1142.
[5] R.M. Melgoza, G. Buitrón, Degradation of *p*-nitrophenol in a batch biofilter under sequential anaerobic/aerobic environments, Water Sci. Technol. 44 (4) (2001) 151–157.
[6] D. Chen, A.K. Ray, Photodegradation kinetics of 4-nitrophenol in TiO_2, suspension, Water Res. 32 (11) (1998) 3223–3234.
[7] B.A. Donlon, E. Razo-Flores, J. Field, G. Lettinga, J. Field, Continuous detoxification, transformation and degradation of nitrophenols in up-flow anaerobic sludge blanket (UASB) reactors, Biotechnol. Bioeng. 51 (1996) 439–444.
[8] K. Karim, S.K. Gupta, Continuous biotransformation and removal of nitrophenols under denitrifying conditions, Water Res. 37 (2003) 2953–2959.
[9] O.A. O'Conner, L.Y. Young, Effects of six different functional groups and their position on the bacterial metabolism of monosubstituted phenols under anaerobic conditions, Environ. Sci. Technol. 30 (5) (1996) 1419–1427.
[10] S.K. Tseng, M.R. Lin, Treatment of organic wastewater by anaerobic biological fludized bed reactor, Water Sci. Technol. 29 (12) (1994) 157–160.
[11] J.G. Bisaillon, F. Lepine, R. Beaudet, M. Sylvestre, Potantial for carboxylation–dehydroxylation of phenolic compounds by a methanogenic consortium, Can. J. Microbiol. 39 (1993) 628–642.
[12] O. Alexander, Biodegradation of organic chemicals, Environ. Sci. Technol. 18 (1985) 106–111.
[13] EPA: Environmental Protection Agency, Ambient water quality for nitrophenols, EPA 440 (1980) 580–063.
[14] J. Iza, E. Colleran, J.M. Paris, W.M. Wu, International workshop on anaerobic treatment technology for municipal and industrial wastewaters: summary paper, Water Sci. Technol. 24 (8) (1991) 1–16.

[15] D.T. Sponza, O.S. Kuscu, *p*-Nitrophenol removal in a sequential anaerobic migrating blanket reactor (AMBR)/aerobic completely stirred tank, reactor (CSTR) system, Process Biochem. 40 (2005) 1679–1691.
[16] R.E. Speece, Anaerobic Biotechnology for Industrial Wastewater, Archae Press, Tennessee, 1996.
[17] APHA-AWWA, Standard Methods for Water a Wastewater, 17th ed., American Public Health Association, Washington, DC, 1992.
[18] A. Oren, P. Garevich, Y. Henis, Reduction of nitrosubstituted aromatic compounds by the halophilic anaerobic eubacteria *Haloanaerobium praevalens* and *Sporohalobacter marismortui*, Appl. Environ. Microbiol. 57 (11) (1991) 3367–3370.
[19] M. Beydilli, L. Paulosathis, W.C. Tincher, Decolorization and toxicity screening of selected reactive azo dye sunder methanogenic conditions, Water Sci. Technol. 38 (4/5) (1998) 225–232.
[20] E. Razo-Flores, M. Luijten, B.A. Donlon, G. Lettinga, J.A. Field, Biodegradation of selected azo dye under methanogenic conditions, Water Sci. Technol. 36 (6/7) (1997) 65–72.
[21] G.K. Anderson, G. Yang, Determination of bicarbonate and total volatile acid concentration in anaerobic digesters using a simple titration, Water Environ. Res. 64 (1992) 53–59.
[22] H. Yu, F. Wilson, J. Tay, Kinetic analysis of an anaerobic filter treating soybean wastewater, Water Res. 32 (11) (1998) 3341–3352.
[23] P. Grau, M. Dohanyas, J. Chudoba, Kinetic of multicomponent substrate removal by activated sludge, Water Res. 9 (1975) 337–342.
[24] I. Oztürk, M. Altinbas, O. Arikan, A. Demir, Anaerobic UASBR treatment of young landfill leachate, in: Proceedings of the First International Workshop on Environmental Quality and Environmental Engineering in the Middle East Region Konya, Turkey, 1996, pp. 1419–1427.
[25] S. Satyanarayan, S.N. Kaul, Kinetics of an anaerobic moving bed reactor system treating synthetic milk wastewater, J. Environ. Sci. Health: Part A Toxic/Hazard. Subst. Environ. Eng. A 37 (9) (2002) 1737–1755.
[26] R.R. Van der Meer, P.M. Heertjes, Mathematical description of anaerobic treatment of wastewater in up-flow reactors, Biotechnol. Bioeng. 25 (11) (1983) 2531–2556.
[27] Y.R. Chen, A.G. Hashimoto, Substrate utilisation kinetic model for biological treatment processes, Biotechnol. Bioeng. 22 (1980) 2081–2095.
[28] K. Han, O. Levenspiel, Extended Monod kinetics for substrate, product and cell inhibition, Biochem. Bioeng. 32 (1988) 403–437.
[29] A.L. Lehninger, The Molecular Basis of Cell Structure and Function Biochemistry, 3rd ed., Word Publishers Inc., New York, 1997, 189–195.
[30] Y. Seungho, L. Semprini, Kinetics and modeling of reductive dechlorination at high PCE and TCE concentrations, Biotechnol. Bioeng. 88 (4) (2004) 451–460.
[31] S.K. Tseng, C.J. Yang, The reaction characteristics of wastewater containing nitrophenol treated using an anaerobic biological fludized bed, Water Sci. Technol. 30 (1994) 233–240.
[32] K. Karim, S.K. Gupta, Biotrasformation of nitrophenols in up-flow anaerobic sludge blanket reactors, Bioresour. Technol. 80 (2001) 179–186.
[33] B.A. Donlon, E. Razo-Flores, J.A. Field, G. Lettinga, Toxicity of *N*-substituted aromatics to acetolastic methanogenic activity in granular sludge, Appl. Environ. Microbiol. 61 (1995) 3889–3893.
[34] O. Kuscu, D.T. Sponza, Performance of anaerobic baffled reactor (ABR) treating synthetic wastewater containing *p*-nitrophenol, Enzyme Microb. Technol. 36 (2005) 888–895.
[35] E. Behling, A. Diaz, G. Colina, M. Herrera, E. Gutierrez, E. Chacin, E. Fernandez, C.F. Forster, Domestic wastewater treatment using a UASB reactor, Bioresource Technol. 61 (1997) 239–245.
[36] K. Karim, S.K. Gupta, Effect of shock and mixed nitrophenolic loadings on the performance of UASB reactors, Water Res. 40 (2006) 935–942.
[37] Z. She, M. Gao, Y. Chen, Toxicity and biodegradation of 2,4 dinitrophenol and 3 nitrophenol in anaerobic system, Water Res. 40 (9) (2005) 3015–3024.
[38] P. Haghighi, S.K. Battacharya, Fate and toxic effects of nitrophenols on anaerobic treatment system, Water Sci. Technol. 34 (5/6) (1996) 345–350.
[39] M.C. Tomei, M.C. Annesini, S. Bussoletti, 4 nitrophenol biodegradation in a SBR reactor: kinetic study time and effect of filling time, Water Res. 38 (2) (2004) 375–384.
[40] S. Zonglian, M. Gao, C. Jin, J. Chen, Toxicity and biodegradation of 2,4 dinitrophenol and 3-nitrophenol in anaerobic systems, Process Biochem. 40 (9) (2005) 3017–3024.
[41] M.R. Podeh, S.K. Bhattacharya, M. Qu, Effects of nitrophenols on acetate utilizing methanogenic systems, Water Res. 29 (2) (1995) 391–399.